arXiv:1106.2360v1 [cond-mat.str-el] 13 Jun 2011

Mass Enhancement in an Intermediate-Valent Regime of Heavy-Fermion Systems

Katsunori Kubo

Advanced Science Research Center, Japan Atomic Energy Agency, Tokai, Ibaraki 319-1195

(Received March 31, 2011; accepted April 18, 2011; published online June 10, 2011)

We study the mechanism of the mass enhancement in an intermediate-valent regime of heavy-fermion materials. We find that the crossovers between the Kondo, intermediate valent, and almost empty f-electron regimes become sharp with the Coulomb interaction between the conduction and f electrons. In the intermediate-valent regime, we find a substantial mass enhancement, which is not expected in previous theories. Our theory may be relevant to the observed nonmonotonic variation in the effective mass under pressure in $CeCu_2Si_2$ and the mass enhancement in the intermediate-valent compounds α-$YbAlB_4$ and β-$YbAlB_4$.

KEYWORDS: mass enhancement, Gutzwiller approximation, extended periodic Anderson model, valence fluctuations, heavy-fermion superconductivity, valence transition

The heavy-fermion phenomenon is one of the most remarkable consequences of a strong electron correlation. In some heavy-fermion materials, the effective mass of electrons becomes a thousand times as large as the free-electron mass. Such heavy electron mass is due to the renormalization effect on the hybridization band by the strong Coulomb interaction U between localized f-electrons.

After the discovery of the superconductivity in the heavy-fermion compound $CeCu_2Si_2$,[1] several heavy-fermion superconductors have been investigated. Since the onsite Coulomb interaction is strong in a heavy-fermion system, superconductivity is expected to be unconventional, i.e., other than the s-wave, and has been one of the central issues in the research field of solid state physics. In many cases, superconductivity takes place around a magnetic quantum critical point, where the magnetic transition temperature becomes absolute zero. Thus, the superconducting pairing interaction is supposed to be mediated by magnetic fluctuations in these systems.

However, in $CeCu_2Si_2$[2] and $CeCu_2Ge_2$,[3] superconducting transition temperatures become maximum in high-pressure regions far away from the magnetic quantum critical points. In addition, the superconducting region splits into two regions in $CeCu_2Si_{1.8}Ge_{0.2}$.[4] Thus, the superconductivity in the high-pressure region in these compounds is difficult to be understood by the magnetic fluctuation scenario, and the superconductivity mediated by valence fluctuations is proposed.[5,6] In these compounds, the effective mass, deduced from specific heat measurements or the temperature dependence of electrical resistivity, decreases rapidly at approximately the pressure where the superconducting transition temperature becomes maximum.[7,8] The effective mass m^* in heavy-electron systems is closely related to the valence of f ions:[9,10]

$$\frac{m^*}{m} = \frac{1 - n_f/2}{1 - n_f}, \tag{1}$$

where m is the free-electron mass and n_f is the number of f electrons per site. This relation is derived for the periodic Anderson model (PAM) with $U \to \infty$ by the Gutzwiller method. Thus, m^* decreases as n_f decreases. In Ce compounds, n_f decreases under pressure, since the f-electron level ϵ_f in a positively charged Ce ion surrounded by negatively charged ions becomes higher and also the hybridization matrix element V increases. Therefore, we expect that a sharp change in n_f or large valence fluctuations play important roles in the superconductivity in these materials.

However, eq. (1) is derived for the ordinary PAM, which does not show a sharp valence change. Moreover, the effective mass has a peak in $CeCu_2Si_2$ under pressure before the superconducting transition temperature becomes maximum.[8] Such a nonmonotonic variation in the effective mass cannot be expected from eq. (1). Note also that, in $CeCu_2Ge_2$, the effective mass shows a shoulder structure before superconducting transition temperature becomes maximum.[7] This shoulder structure may also become a peak if we can subtract the contributions of magnetic fluctuations, which are large in the low-pressure region. These peak structures may be explained by a combined effect of valence fluctuations and the renormalization described by eq. (1),[8] but the applicability of eq. (1) to a model with large valence fluctuations is not justified. Thus, we should extend eq. (1) to a model that shows a sharp valence change to understand the superconductivity in $CeCu_2Si_2$ and $CeCu_2Ge_2$ coherently by the valence fluctuation scenario.

Another important recent issue on the heavy-fermion phenomenon is the heavy-fermion behavior in the intermediate-valent compounds α-$YbAlB_4$ and β-$YbAlB_4$.[11] β-$YbAlB_4$ is reported to show superconductivity at a very low temperature.[12] Although both compounds show heavy-fermion behavior, the valences of Yb ions are +2.73 for α-$YbAlB_4$ and +2.75 for β-$YbAlB_4$.[13] Thus, the hole numbers in the f level are $n_f = 0.73$ and 0.75 for α-$YbAlB_4$ and β-$YbAlB_4$, respectively. With such $n_f \ll 1$, heavy-fermion behavior is not expected from eq. (1).

In this research, we study an extended periodic Anderson model (EPAM) with the Coulomb interaction U_{cf} between the conduction and f electrons, which induces sharp valence transitions, by the Gutzwiller method. We extend the Gutzwiller method for the PAM developed by Fazekas and Brandow[10] to the present model. This extension is straightforward but the formulation is lengthy, and here we show only the obtained results. The details of the derivation will be reported elsewhere. Although the EPAM has been investigated by some numerical methods in recent years,[14–16] the effect of U_{cf} on the mass enhancement is not yet clarified well.

The EPAM is given by[17)]

$$
\begin{aligned}
H = \sum_{\boldsymbol{k}\sigma} \epsilon_{\boldsymbol{k}} c^{\dagger}_{\boldsymbol{k}\sigma} c_{\boldsymbol{k}\sigma} + \epsilon_f \sum_{i\sigma} n_{fi\sigma} - V \sum_{\boldsymbol{k}\sigma} (f^{\dagger}_{\boldsymbol{k}\sigma} c_{\boldsymbol{k}\sigma} + \text{h.c.}) \\
+ U \sum_{i} n_{fi\uparrow} n_{fi\downarrow} + U_{cf} \sum_{i\sigma\sigma'} n_{ci\sigma} n_{fi\sigma'},
\end{aligned}
\tag{2}
$$

where $c_{\boldsymbol{k}\sigma}$ and $f_{\boldsymbol{k}\sigma}$ are the annihilation operators of the conduction and f electrons, respectively, with the momentum $\boldsymbol{k}$ and the spin σ. $n_{ci\sigma}$ and $n_{fi\sigma}$ are the number operators at site i with σ of the conduction and f electrons, respectively. $\epsilon_{\boldsymbol{k}}$ is the kinetic energy of the conduction electron. In the following, we set the energy level of the conduction band as the origin of energy, i.e., $\sum_{\boldsymbol{k}} \epsilon_{\boldsymbol{k}} = 0$. We set $U \to \infty$, since the Coulomb interaction between well-localized f electrons is large.

We consider the variational wave function given by $|\psi\rangle = P_{ff} P_{cf} |\phi\rangle$, where $P_{ff} = \prod_i [1 - n_{fi\uparrow} n_{fi\downarrow}]$ excludes the double occupancy of f electrons at the same site, and $P_{cf} = \prod_{i\sigma\sigma'} [1 - (1-g) n_{ci\sigma} n_{fi\sigma'}]$ is introduced to deal with the on-site correlation between conduction and f electrons.[14)] g is a variational parameter. The one-electron part of the wave function is given by $|\phi\rangle = \prod_{k<k_{\rm F},\sigma} [c^{\dagger}_{\boldsymbol{k}\sigma} + a(\boldsymbol{k}) f^{\dagger}_{\boldsymbol{k}\sigma}] |0\rangle$, where $k_{\rm F}$ is the Fermi momentum, $|0\rangle$ denotes vacuum, and $a(\boldsymbol{k})$ is determined variationally. Here, we have assumed that the number of electrons n per site is smaller than 2.

Then, we apply Gutzwiller approximation. Here, we introduce the quantity $d_{c\sigma} = \sum_i \langle n_{ci\sigma}(n_{fi\uparrow} + n_{fi\downarrow}) \rangle / L$, where $\langle \cdots \rangle$ denotes the expectation value and L is the number of lattice sites. In evaluating expectation values by Gutzwiller approximation, we determine $d_{c\sigma}$, which has the largest weight in summations. The result is $g^2 = [d_{c\sigma}(1 - n_f - n_{c\sigma} + d_{c\sigma})]/[(n_f - d_{c\sigma})(n_{c\sigma} - d_{c\sigma})]$, where $n_{c\sigma} = \sum_i \langle n_{ci\sigma} \rangle / L$ and $n_f = \sum_\sigma n_{f\sigma} = \sum_{i\sigma} \langle n_{fi\sigma} \rangle / L$. This is the same form as that in the Hubbard model,[18)] if we regard $n_{c\sigma}$ as $n^{\rm H}_{\sigma}$, n_f as $n^{\rm H}_{\bar{\sigma}}$, and $d_{c\sigma}$ as $d^{\rm H}$, where $n^{\rm H}_{\sigma}$ and $d^{\rm H}$ are the numbers of σ-spin electrons and doubly occupied sites per lattice site, respectively, in the Hubbard model, and $\bar{\sigma}$ denotes the opposite spin of σ.

In the following, we assume a paramagnetic state, i.e., $n_{f\sigma} = n_f/2$, $n_{c\sigma} = n_c/2 = (n - n_f)/2$, and $d_{c\sigma} = d/2$, and optimize the wave function so that it has the lowest energy. In the following, we regard d as a variational parameter instead of g as is done in ordinary Gutzwiller approximation. Then we find that $a(\boldsymbol{k}) = 2\tilde{V}_1 / \{\tilde{\epsilon}_f - \tilde{\epsilon}_{\boldsymbol{k}} + [(\tilde{\epsilon}_f - \tilde{\epsilon}_{\boldsymbol{k}})^2 + 4\tilde{V}_2^2]^{1/2}\}$, where $\tilde{V}_2 = \sqrt{q}\tilde{V}_1 = \sqrt{q} \times q_{cf} V$ and $\tilde{\epsilon}_{\boldsymbol{k}} = q_c \epsilon_{\boldsymbol{k}}$. $\tilde{\epsilon}_f$ is the renormalized f-level obtained by solving integral equations, as we will show later. The renormalization factors are given by $q = [n_f^2 (n_c - d)(1 - n_c/2)(1 - n_f - n_c/2 + d/2)]/[(1 - n_f/2)(1 - n_f) n_c (n_f - d/2)^2]$, $q_{cf} = \big(1 + \{d(n_c - d)/[(n_f - d/2)(1 - n_f - n_c/2 + d/2)]\}^{1/2}/2\big)(n_f - d/2)^2/[n_f^2(1 - n_c/2)]$, and $q_c = q_{c\sigma} = \{[(n_{c\sigma} - d_{c\sigma})(1 - n_f - n_{c\sigma} + d_{c\sigma})]^{1/2} + [d_{c\sigma}(n_f - d_{c\sigma})]^{1/2}\}^2/[n_{c\sigma}(1 - n_{c\sigma})]$. $q_{c\sigma}$ has the same form as the renormalization factor $q^{\rm H}_{\sigma}$ in the Hubbard model[18)] as for the Gutzwiller parameter g.

To determine n_f, $\tilde{\epsilon}_f$, and d, we solve the following integral equations. $n_f = n/2 + I_3$, $\epsilon_f - \tilde{\epsilon}_f = -2\tilde{V}_2^2 I_2 q \partial q^{-1}/\partial n_f - (I_1 - I_4 - I_3\tilde{\epsilon}_f) q_c^{-1} \partial q_c/\partial n_f + 4\tilde{V}_2^2 I_2 q_{cf}^{-1} \partial q_{cf}/\partial n_f$, and $U_{cf} = -2\tilde{V}_2^2 I_2 q \partial q^{-1}/\partial d - (I_1 - I_4 - I_3\tilde{\epsilon}_f) q_c^{-1} \partial q_c/\partial d + 4\tilde{V}_2^2 I_2 q_{cf}^{-1} \partial q_{cf}/\partial d$. The integrals are given by $I_1 = \sum_{k<k_{\rm F}} \tilde{\epsilon}_{\boldsymbol{k}}/L$, and $I_l = \sum_{k<k_{\rm F}} \{(\tilde{\epsilon}_{\boldsymbol{k}} - \tilde{\epsilon}_f)^{l-2}/[(\tilde{\epsilon}_{\boldsymbol{k}} - \tilde{\epsilon}_f)^2 + 4\tilde{V}_2^2]^{1/2}\}/L$ for $l = 2$–4. The total energy per site is $I_1 + n_f\epsilon_f + (n/2 - n_f)\tilde{\epsilon}_f - I_4 - 4\tilde{V}_2^2 I_2 + U_{cf} d$.

We can evaluate expectation values of physical quantities in the optimized wave function. Here, we consider the jump in the electron distribution at the Fermi level; the inverse of the jump corresponds to the mass enhancement factor. The jump in $n_c(\boldsymbol{k}) = \langle c^{\dagger}_{\boldsymbol{k}\sigma} c_{\boldsymbol{k}\sigma} \rangle$ at the Fermi level is given by $\Delta n_c(k_{\rm F}) = q_c/[1 + qa^2(k_{\rm F})]$. The jump in $n_f(\boldsymbol{k}) = \langle f^{\dagger}_{\boldsymbol{k}\sigma} f_{\boldsymbol{k}\sigma} \rangle$ is given by $\Delta n_f(k_{\rm F}) = q_f q a^2(k_{\rm F})/[1 + qa^2(k_{\rm F})]$. The renormalization factor q_f for an f electron is given by $q_f = q_f^{(c\uparrow)} q_f^{(c\downarrow)} (1 - n_f)/(1 - n_f/2)$, where $q_f^{(c\sigma)} = \{[(n_f - d_{c\sigma})(1 - n_f - n_{c\sigma} + d_{c\sigma})]^{1/2} + [d_{c\sigma}(n_{c\sigma} - d_{c\sigma})]^{1/2}\}^2/[n_f(1 - n_f)]$. $q_f^{(c\sigma)}$ has the same form as $q^{\rm H}_{\sigma}$ in the Hubbard model,[18)] if we regard n_f as $n^{\rm H}_{\sigma}$, $n_{c\sigma}$ as $n^{\rm H}_{\bar{\sigma}}$, and $d_{c\sigma}$ as $d^{\rm H}$. In the following, we call $1/\Delta n(k_{\rm F}) = 1/[\Delta n_c(k_{\rm F}) + \Delta n_f(k_{\rm F})]$ the mass enhancement factor.

Before presenting our calculated results, here we consider three extreme cases in the model. First, we consider a case with a positively large ϵ_f. In this case, $n_f \simeq 0$ and the energy is almost the same as the kinetic energy of the free conduction band with $n_c = n$. Second, we consider a case with a negative ϵ_f with a large magnitude. In this case, $n_f \simeq 1$ and $n_c \simeq n - 1$. The energy is approximately given by the sum of $L[\epsilon_f + (n-1)U_{cf}]$ and the kinetic energy of the free conduction band with $n_c = n - 1$. We call this regime the Kondo regime. From the form of the renormalization factors and $a(\boldsymbol{k})$, the mass enhancement factor becomes large as $n_f \to 1$, which is consistent with the previous result on the PAM. Third, we consider a case with an intermediate ϵ_f with a large U_{cf}. In this case, the f and conduction electrons tend to avoid each other, and thus $n_f + n_c/2 \simeq 1$ and $d \simeq 0$. That is, $n_f \simeq 2 - n$ and $n_c \simeq 2n - 2$. Here, we call this regime the intermediate-valent regime. In this case, both the f and conduction electrons are almost localized, and the energy is approximately $L(2 - n)\epsilon_f$. In this intermediate-valent regime, the mass enhancement factor becomes large as $n_f + n_c/2 \to 1$ and $d \to 0$. This mass enhancement in the intermediate-valent regime is not realized in the ordinary PAM and is a result of the effect of U_{cf}.

In the following, we consider a simple model of the kinetic energy: the density of states per spin is given by $\rho(\epsilon) = 1/(2W)$ for $-W \le \epsilon \le W$; otherwise, $\rho(\epsilon) = 0$.

Now, we show our calculated results. Figure 1(a) shows n_f as a function of ϵ_f for several values of U_{cf} for $V/W = 0.1$ and $n = 1.25$. For a large U_{cf}, we recognize the three regimes mentioned above. A first-order phase transition occurs from the intermediate-valent regime to the $n_f \simeq 0$ regime for $U_{cf}/W > 1.24$. We observe hysteresis by increasing and decreasing ϵ_f across the first-order phase transition point, and here we show the values of the state that has the lower energy. Figure 1(b) shows the valence susceptibility $\chi_{\rm V} = -{\rm d}n_f/{\rm d}\epsilon_f$ as a function of ϵ_f. The valence susceptibility enhances around the boundaries of three regimes for a large U_{cf}. For a small U_{cf}, such a boundary is not clear and $\chi_{\rm V}$ has a broad peak. Figure 1(c) shows the mass enhancement factor $1/\Delta n(k_{\rm F})$ as a function of ϵ_f. In addition to the enhancement for $n_f \to 1$ as in the ordinary PAM, we find another region, that is, the intermediate-valent regime $n_f \simeq 2 - n$, in which the mass enhancement factor becomes large. This enhancement, particularly, a peak as a function of ϵ_f, is not expected for the PAM without U_{cf}. The large effective mass in the intermediate-valent compounds α-YbAlB$_4$ and β-YbAlB$_4$

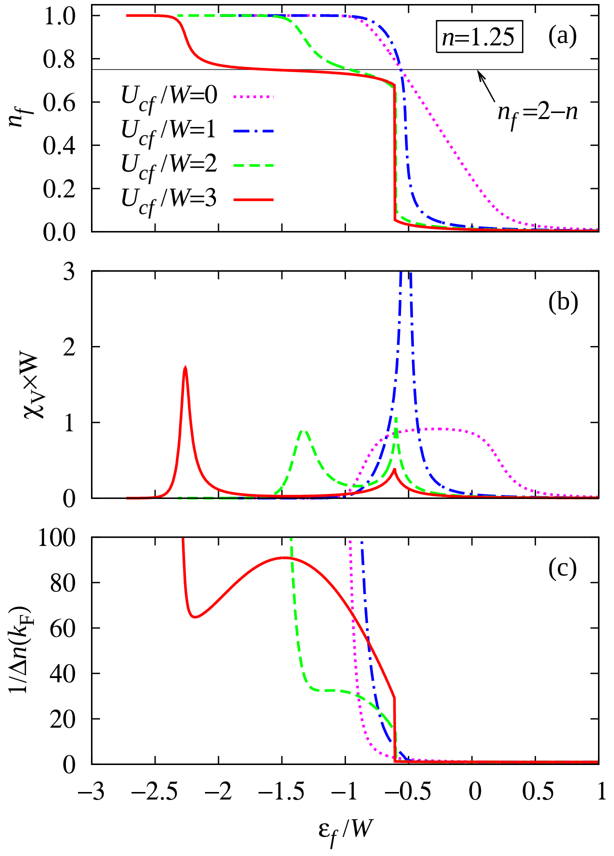

Fig. 1. (Color online) ϵ_f dependences of (a) n_f, (b) χ_V, and (c) $1/\Delta n(k_F)$ for $V/W = 0.1$ and $n = 1.25$. $U_{cf}/W = 0$ (dotted lines), 1 (dash-dotted lines), 2 (dashed lines), and 3 (solid lines).

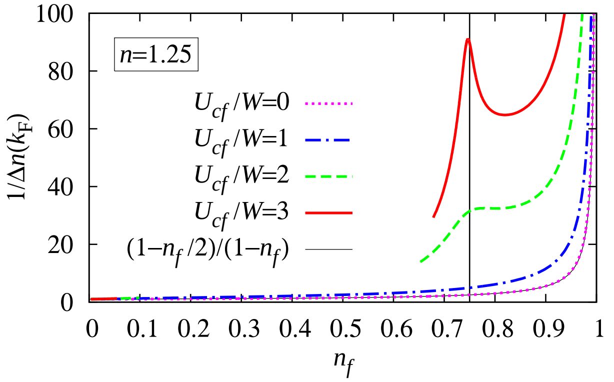

Fig. 2. (Color online) $1/\Delta n(k_F)$ as a function of n_f for $V/W = 0.1$ and $n = 1.25$. $U_{cf}/W = 0$ (dotted line), 1 (dash-dotted line), 2 (dashed line), and 3 (solid line). The thin line is $(1 - n_f/2)/(1 - n_f)$. The vertical line indicates $n_f = 2 - n$.

and the nonmonotonic variation in the effective mass under pressure in $CeCu_2Si_2$ may be explained by the present theory.

To clearly observe the effect of U_{cf} on the mass enhancement, we show $1/\Delta n(k_F)$ as a function of n_f in Fig. 2. The thin line, which is almost overlapping with the $U_{cf} = 0$ data, represents the mass enhancement factor $(1 - n_f/2)/(1 - n_f)$ obtained for the PAM with $U_{cf} = 0$ and $g = 1$. By increasing U_{cf}, $1/\Delta n(k_F)$ becomes large, particularly in the intermediate-valent regime $n_f \simeq 2 - n$.

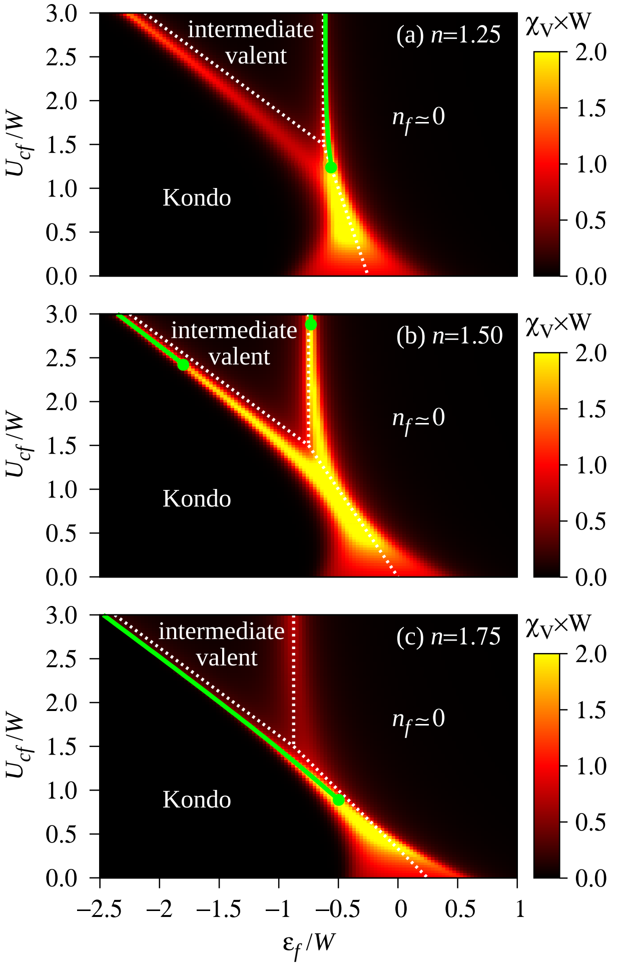

Fig. 3. (Color online) χ_V as a function of ϵ_f and U_{cf} with $V/W = 0.1$ for (a) $n = 1.25$, (b) $n = 1.50$, and (c) $n = 1.75$. The solid lines represent the first-order valence transition lines. The solid circles denote the critical points of the valence transition. The dotted lines indicate crossover lines determined by comparing the energies of the three extreme states (see text).

In Fig. 3, we show the valence susceptibility χ_V as a function of ϵ_f and U_{cf} for $n = 1.25$, 1.50, and 1.75. In this figure, we also draw the first-order valence transition lines and their critical points. The crossover lines, represented by the dotted lines, are determined by comparing the energies of the three extreme states: $n_f = 0$, $n_f = 1$, and $n_f + n_c/2 = 1$ with $d = 0$. The region where χ_V becomes large is captured well by the crossover lines obtained by such a simple consideration. For $n = 1.25$, the first-order valence transition occurs only from the intermediate-valent regime to $n_f \simeq 0$ regime, while for $n = 1.75$ it occurs only between the Kondo and intermediate-valent regimes, within the U_{cf} range presented here. n_f in the intermediate-valent regime differs between these two cases: $n_f \simeq 0.75$ for $n = 1.25$ and $n_f \simeq 0.25$ for $n = 1.75$. The first-order transition seems to occur easily between very different states, that is, a crossover accompanying a large valence change tends to become a first-order phase transition. Between these two cases, for $n = 1.50$, both the transitions take place for $U_{cf}/W > 2.88$. Note that, since only the $n = 1.75$ case is well investigated in previous studies,[14–16] the first-order transition between the intermediate valent and $n_f \simeq 0$ regimes has not been elucidated.

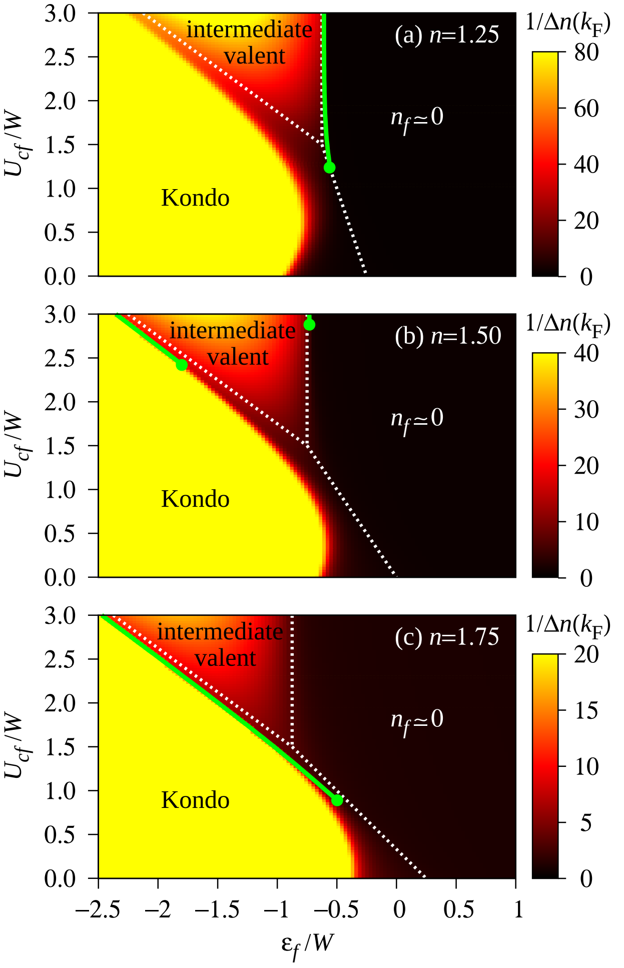

Fig. 4. (Color online) $1/\Delta n(k_\mathrm{F})$ as a function of ϵ_f and U_{cf} with $V/W = 0.1$ for (a) $n = 1.25$, (b) $n = 1.50$, and (c) $n = 1.75$. The lines and circles are the same as those in Fig. 3.

Figure 4 shows the mass enhancement factor $1/\Delta n(k_\mathrm{F})$ as a function of ϵ_f and U_{cf}. A large mass enhancement occurs in the intermediate-valent regime in addition to the Kondo regime. Here, we note that the large mass enhancement occurs in the middle of the intermediate-valent regime. Thus, this enhancement is not due to the valence fluctuations. In $\mathrm{CeCu_2Si_2}$, the effective mass has a peak before the superconducting transition temperature becomes maximum under pressure. If the system is in the Kondo regime at ambient pressure, passes the intermediate-valent regime under pressure, and finally reaches near a critical point, it is consistent with our theory provided the pairing interaction of superconductivity is mediated by the valence fluctuations. Such a situation can be realized, for example, for $n = 1.5$ as is shown in Fig. 4(b). A similar discussion may also be applicable to $\mathrm{CeCu_2Ge_2}$ if we can subtract the contributions of the magnetic fluctuations.

In summary, we have studied the extended periodic Anderson model with U_{cf} by Gutzwiller approximation. We have found that three regimes, that is, the $n_f \simeq 0$, intermediate valent, and Kondo regimes, are clearly defined for a large U_{cf}. Then, we have found that, in the intermediate-valent regime, the effective mass is enhanced substantially. According to the present theory, the large mass enhancement in the intermediate-valent regime indicates a large U_{cf}. Thus, our theory provides helpful information for searching a superconductor with valence-fluctuation-mediated pairing.

---

1) F. Steglich, J. Aarts, C. D. Bredl, W. Lieke, D. Meschede, W. Franz, and H. Schäfer: Phys. Rev. Lett. **43** (1979) 1892.
2) B. Bellarbi, A. Benoit, D. Jaccard, J. M. Mignot, and H. F. Braun: Phys. Rev. B **30** (1984) 1182.
3) E. Vargoz and D. Jaccard: J. Magn. Magn. Mater. **177–181** (1998) 294 .
4) H. Q. Yuan, F. M. Grosche, M. Deppe, C. Geibel, G. Sparn, and F. Steglich: Science **302** (2003) 2104.
5) K. Miyake, O. Narikiyo, and Y. Onishi: Physica B **259–261** (1999) 676.
6) Y. Onishi and K. Miyake: J. Phys. Soc. Jpn. **69** (2000) 3955.
7) D. Jaccard, H. Wilhelm, K. Alami-Yadri, and E. Vargoz: Physica B **259–261** (1999) 1.
8) A. T. Holmes, D. Jaccard, and K. Miyake: Phys. Rev. B **69** (2004) 024508.
9) T. M. Rice and K. Ueda: Phys. Rev. B **34** (1986) 6420.
10) P. Fazekas and B. H. Brandow: Phys. Scr. **36** (1987) 809.
11) R. T. Macaluso, S. Nakatsuji, K. Kuga, E. L. Thomas, Y. Machida, Y. Maeno, Z. Fisk, and J. Y. Chan: Chem. Mater. **19** (2007) 1918.
12) S. Nakatsuji, K. Kuga, Y. Machida, T. Tayama, T. Sakakibara, Y. Karaki, H. Ishimoto, S. Yonezawa, Y. Maeno, E. Pearson, G. G. Lonzarich, L. Balicas, H. Lee, and Z. Fisk: Nat. Phys. **4** (2008) 603.
13) M. Okawa, M. Matsunami, K. Ishizaka, R. Eguchi, M. Taguchi, A. Chainani, Y. Takata, M. Yabashi, K. Tamasaku, Y. Nishino, T. Ishikawa, K. Kuga, N. Horie, S. Nakatsuji, and S. Shin: Phys. Rev. Lett. **104** (2010) 247201.
14) Y. Onishi and K. Miyake: Physica B **281–282** (2000) 191.
15) S. Watanabe, M. Imada, and K. Miyake: J. Phys. Soc. Jpn. **75** (2006) 043710.
16) Y. Saiga, T. Sugibayashi, and D. S. Hirashima: J. Phys. Soc. Jpn. **77** (2008) 114710.
17) C. E. T. Gonçalves da Silva and L. M. Falicov: Solid State Commun. **17** (1975) 1521 .
18) M. C. Gutzwiller: Phys. Rev. **137** (1965) A1726.